IOP Conf. Series: Journal of Physics: Conf. Series **1425** (2020) 012122 doi:10.1088/1742-6596/1425/1/012122

Modelling Fluidic Windows for Heating and Cooling

Mathias Fraaß[1] **and Lingqi Su**[1,2]

[1]Laboratory for Electrical, Measurement and Control Technology in Buildings, Beuth University of Applied Sciences Berlin, Berlin/Germany

[2]Otto-Schott-Institute of Material Research, Friedrich-Schiller-University Jena, Jena/Germany

Abstract. Recently, we introduced a transparent capillary glass panel fabricated by lamination of a structured glass sheet and a thin glass cover used for liquid circulation. Major applications of such device are room heating and cooling and energy harvesting for heat pumps. In order to model a façade of a building, a story of a building or even the entire building, simplified but accurate models for the temperature and the fluid flow distribution within the capillary panel as well as a device optical and thermal model are necessary. In this paper, our simplified models are introduced.

1. Introduction

Thermal activated surfaces, also known as thermo-active building system (TABS) in some literatures, are useful in room air conditioning with low temperature differences between surface and room, thus advantageous for thermal comfort and energy efficiency of the central heater or chiller involved, especially of heat pumps [1]. In cases when neither floor nor ceiling can be used as thermal activated surfaces, window comes into consideration. In multi-story buildings, the window is also suitable for energy harvesting for heat pumps - rsp. as a sink for heat pumps in reversed operation mode. For these purposes, a transparent capillary glass panel was developed, fabricated by lamination of a structured glass sheet and a thin glass cover used for liquid circulation [2]. **Figure 1** shows the proportion of the windows related to the cover surfaces of rooms (a) and entire buildings (b).

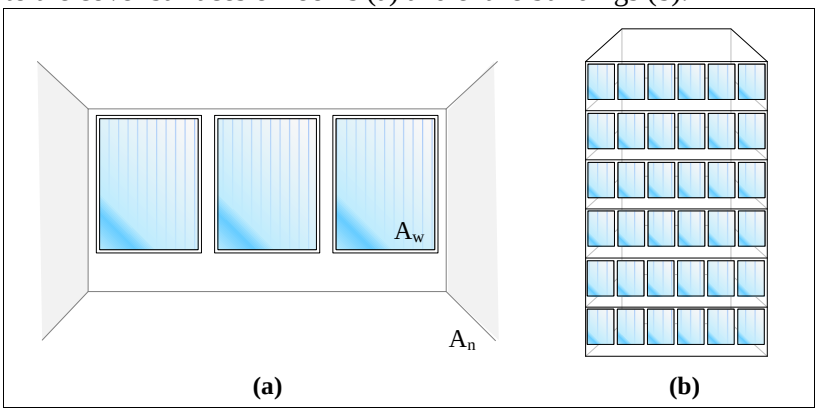

Figure 1. proportions of window area in single rooms (a) and in multi-story buildings (b)

In triple glazed windows, either application can be realized simultaneously by replacing the passive glass panel with the capillary glass, as **Figure *2*** shows. Located at Panel 3 in **Figure *2*** (a), which is

the inner panel of the window, the capillary structure can be used for room heating and cooling. Located at Panel 1 as in **Figure *2*** (b), which is the outer panel of the window, it serves as a heat exchanger opening up the ambient air as a source for a heat pump rsp. as a sink in reversed operation mode. **Figure *2*** (c) shows both use application combined, which means that in the heating case heat is transported from the ambient air into the room and into the opposite direction in the cooling case. In this case, Panel 2 serves as a thermal insulation between Panel 1 und Panel 3 and Surface 2 and Surface 5 can be coated with low-ε material to minimize the heat flow through the window.

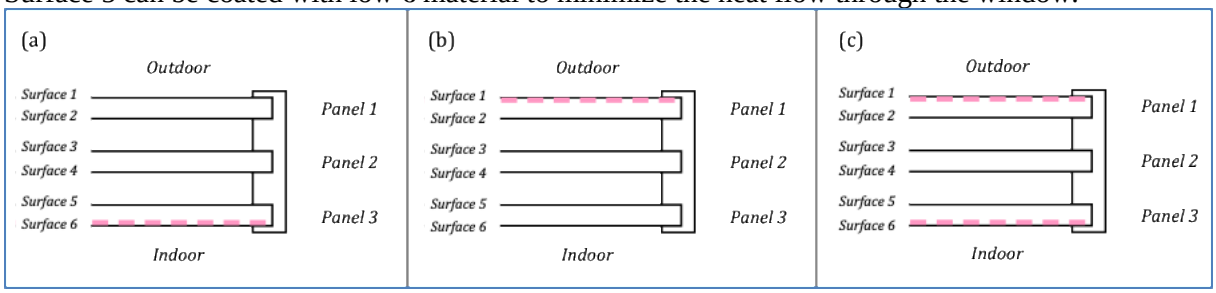

Figure 2. different application and the position of the thermal activated glass panel [1]

Various geometries of the capillary fluid channel have been investigated. Finally, a symmetric trapezoid geometry was selected, as shown in **Figure *3* (a)**. The underlying glass panel is manufactured by a roller with a trapezoid surface. Due to the symmetry of the geometry, the displaced molten glass fits into the gaps between the capillary fluid channels. Afterwards, float glass is laminated onto the rolled glass. The detailed geometry of the capillary glass panel is decribed in [2]. At the both ends of the capillary fluid channel, a supply distributor and a return collector are installed, as shown in **Figure *3* (b)**. The distributor and the collector are described with "stem" in terms of capillary tube technology. The stems are connected with fluid system, forming a fluid circuit, in which the windows are installed parallel to each other to limit the pressure drop, as shown in **Figure *3* (c)**.

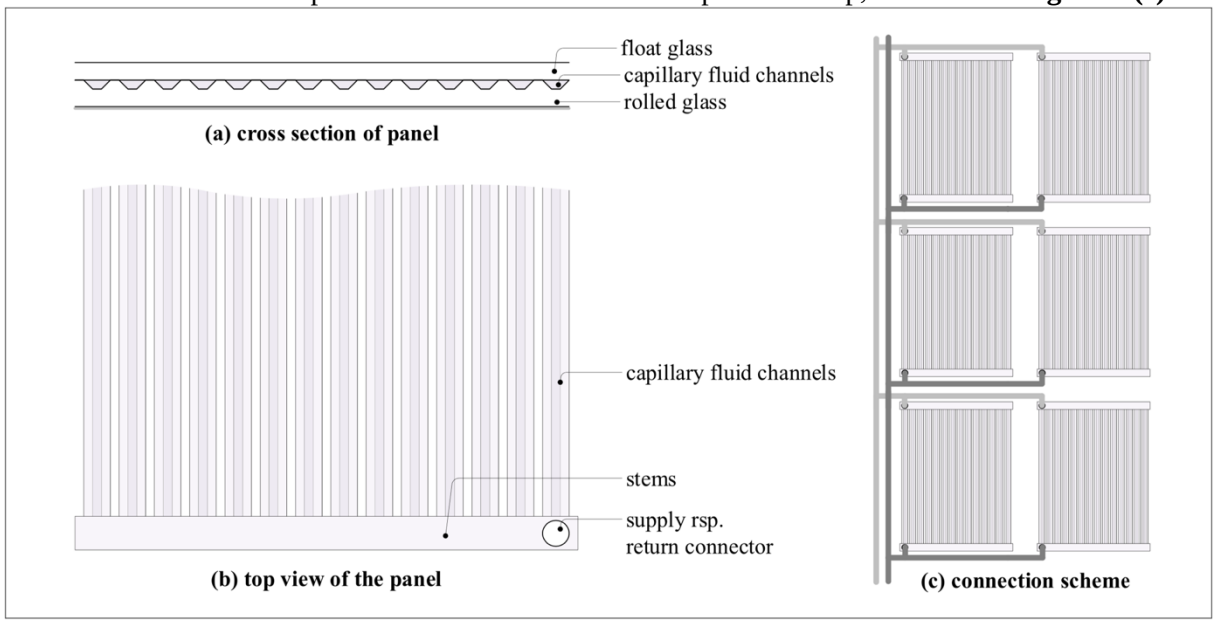

Figure 3. geometry and connection scheme of thermal activated glass panel

To simulate the performance of the device and evaluate the energy efficiency of heater or chiller, it's necessary to develop calculation models for this device and to combine this model with other room, heat or chiller models. During the simulation, each window must be calculated separately taking account of the varying heating and cooling performance in different rooms. Within each window, the distribution of fluid flow rates and the temperature field needs to be determined. A relatively high accuracy of the model is required due to the danger of either freezing or stagnation due to increased viscosity of the fluid in the device.

Because of not only the desirable precision of the simulation but also the complexity of the combined room, heater and chiller model, it is not practicable to use high resolution FEM tools for the simulation. Instead, a simplified but precise model of the single window is needed which can be easily upscaled. The following steps have been made to achieve this goal:

- calculate the two-dimensional temperature field in cross sections of the glass panel as precisely as possible,
- establish a one-dimensional simplified model for the two-dimensional heat conduction inside the glass panel, and
- model the temperature and flow rate distribution inside the window with a limited set of equations

Fortunately, all of these steps require only a stationary treatment. Dynamic aspects can be neglected for the windows and the net, since the heat capacity of the connected building structure overweighs all other capacities to a large extent. Therefore, the windows and the net can be calculated quasi-stationary.

2. Calculating the two-dimensional temperature field with BEM

To calculate the two-dimensional temperature field, the boundary element method (BEM) has been applied. Unlike the finite element method (FEM), the BEM does not require discretization of the whole domain. Instead, it's based on discretized boundary to calculate an integral equation derived from Green's identity [3] [4]. For two-dimensional Laplace's equation, the boundary integral equation is

$$t(p) = \frac{1}{\eta(p)} \oint \frac{dt(q)}{dn} \ln|p-q| - t(q) \frac{\partial}{\partial n} \ln|p-q| \, dq. \tag{1}$$

Here p is a point inside the domain or in any part of the boundary including corners and q is a point on the boundary which serves as the integration variable in the closed line integral. After boundary discretization, the closed line integral turns into an integral over the different boundary elements, giving an approximated temperature field $\tilde{t}$ as

$$\tilde{t}(p) = \frac{1}{\eta(p)} \sum_{i=1}^{n} \left(\frac{\partial}{\partial n} \, t_i \int \ln|q_i - q| \, dq \; - t_i \int \frac{\partial}{\partial n} \ln|q_i - q| \; dq \right). \tag{2}$$

Applying the collocation method, this integral is calculated for q_i as the midpoints of each of the n boundary elements giving the temperature t_j of the jth element as

$$t_j = \frac{1}{\pi} \sum_{i=1}^{n} \left(\frac{\partial}{\partial n} \, t_i \int_i \ln|q_i - q| \, dq \; - t_i \int_i \frac{\partial}{\partial n} \ln|q_i - q| \, \mathrm{d}q \right). \tag{3}$$

$\eta(p)$ is replaced by π, which is the solution of $\eta(p)$ for a point lying on a smooth part of the boundary as this is the case for every midpoint. Since one of the n temperatures t_i in the sum is t_j itself, it leads to a matrix representation

$$A \, \underline{t}' - B \, \underline{t} - \pi \, \underline{t} = 0. \tag{4}$$

Here, $\underline{t}$ is the vector of the n temperatures t_j and $\underline{t}'$ the vector of the n normal derivatives of the temperature field pointing to the interior of the boundary. A and B are matrices with elements

$$a_{j,i} = \int_i \ln|q_i - q| \, dq \tag{5}$$

and

$$b_{j,i} = \int_i \frac{\partial}{\partial n} \ln|q_i - q| \, \mathrm{d}q. \tag{6}$$

Figure 4 shows parameters of the geometry of the thermal activated panel (a) and the BEM calculation model (b). In order to avoid parallel facing exterior straight lines at the duct, which will cause miscalculation, the domain is divided into two subdomains with boundaries ∂B_1 and ∂B_2.

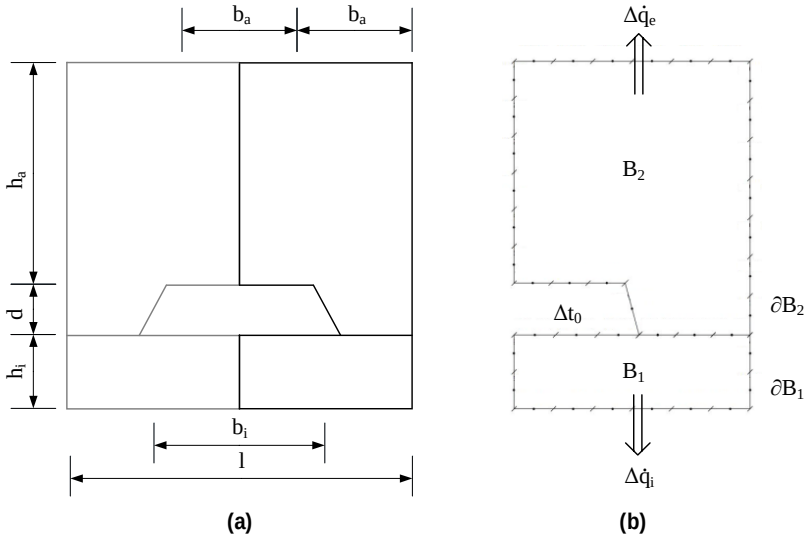

Figure 4. geometry of (a) the heat conducting area and (b) related BEM model

The accuracy of the BEM has been widely validated with known analytical solutions [4]. The number of the necessary boundary elements can be found with convergence investigations. Nowadays, FEM programs are as precise as BEM, but there are still advantages from using BEM [8].

The solution of equation (4) delivers all temperatures and normal derivatives of the boundary. Therefore, the desired heat flux $\Delta\dot{q}_i$ and $\Delta\dot{q}_e$ at both surfaces of the panel are given directly. There is no need to calculate further temperatures inside the domain.

Moreover, BEM is especially advantageous if the equation solving needs to be repeated for several different boundary conditions. The main calculation effort is spent on calculating the matrices A and B. As can be seen in equation (4) and (5), they are only dependent on geometrical parameters. Once these matrices are determined for a single geometry, they can be used for any boundary conditions in this geometry.

3. Establishing a one-dimensional simplified model

Thermal activated surfaces came up in the early 20th century mainly as heating ceilings with embedded tubes. Originally it was thought that the heating performance of theses ceilings would be proportional to the tube interval, similarly to the distance l in **Figure *4***. However, this turned out to be wrong: some ceilings could not reach the predicted performance in practice. This caused a demand of analytical approximate solutions for the heat conduction inside the embedding.

One of these approximate solutions is the well-known rod theory by Kalous [5] based on the analytical solution for the heat conduction in a rod with radiation at both sides (see for instance [6]). **Figure 5 (a)** shows the original stationary problem of a rod with diameter d, length s and adiabatic boundary condition at its end $x = s$. Δt is the temperature difference between the rod and its environment. On the left end of the rod Δt is Δt_0. α_i and α_e are the heat transfer coefficients at both sides of the rod- in [5] referred to as radiation. λ is the thermal conductivity in the rod. The heat flow inside the rod is assumed to be one-dimensional in horizontal direction, which means that there is no temperature difference between both sides of the rod.

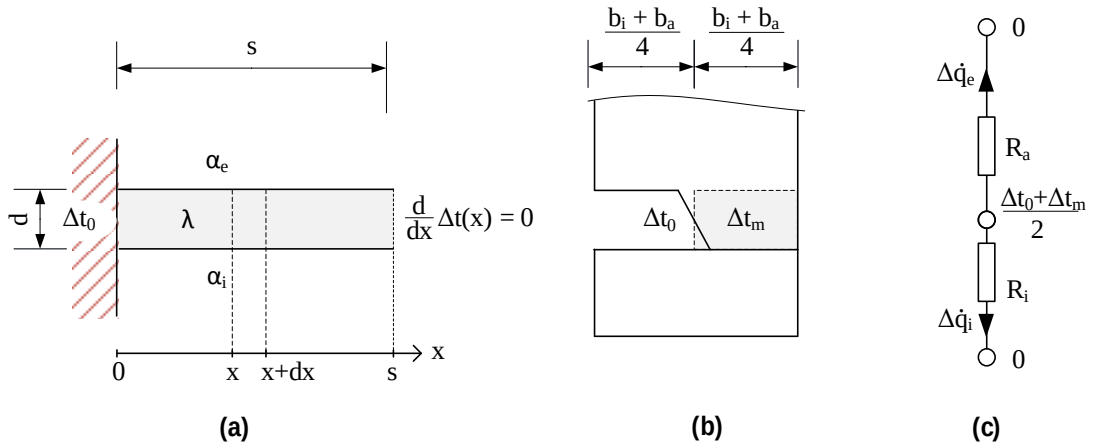

Figure 5. rod theory for thermal activated slabs

In the rod element d*x*, the stationary energy balance is

$$\lambda\, d\, \frac{d}{dx}\Delta t(x) = \lambda\, d\, \frac{d}{dx}\Delta t(x + \mathrm{d}x) + dx\, (\alpha_i + \alpha_e)\, \Delta t(x)\,. \tag{7}$$

This leads to a differential equation

$$\frac{d^2}{dx^2}\Delta t(x) = -\frac{\alpha_i + \alpha_e}{\lambda\, d}\, \Delta t(x),\ \Delta t(0) = \Delta t_0,\ \frac{\mathrm{d}\Delta t}{\mathrm{d}x}(s) = 0\,. \tag{8}$$

with

$$m = \left(\frac{\alpha_i + \alpha_e}{\lambda\, d}\right)^{\frac{1}{2}}. \tag{9}$$

The solution of the problem is

$$\Delta t(x) = \Delta t_0\, \frac{\cosh[m\,(h - x)]}{\cosh mh} \tag{10}$$

delivering the mean temperature difference Δt_m between the rod and its environment as

$$\Delta t_m = \frac{1}{h}\int_0^h \Delta t(x)\,\mathrm{dx} = \frac{\tanh m\,h}{m\,h}\, \Delta t_0 = \eta\, \Delta t_0\,, \tag{11}$$

where η is called the rod coefficient.

Figure 5 (b) shows, how the rod theory fits into the heat conduction problem of the thermal activated glazing. Due to the symmetry of the geometry, both the length of the rod and the length of its root are $(b_i + b_a)/4$. With the thermal resistances R_i and R_e on both sides of the rod, α_i is now $1/R_i$ and $\alpha_a = 1/R_e$. As just mentioned, h becomes now $(b_i + b_a)/4$.

Therefore, the two-dimensional heat conduction problem inside the glass panel is now transformed into a one-dimensional calculation as shown in **Figure 5 (c)**. Again, due to the symmetry, the mean temperature between both sides of the glazing is the average value of Δt_0 and Δt_m.

Table 1 shows the accuracy comparison for a calculation example with the rod theory and the BEM. In this example, it's assumed that the heat conductivity of the glass is 1 W/(m K). The heat transfer coefficient α_i is assumed to be 8 W/(m^2 K). The heat transfer coefficient α_e is 0.8 W/(m^2 K), which corresponds to the thermal resistance between the inner glass panel and the outdoor air in a triple glazed window with 2 low-ε coatings [1]. It is interesting to see that the deviation of this calculation to the highly precise BEM simulation is in terms of $\Delta \dot{q}_i$ and $\Delta \dot{q}_e$ less than 1 percent.

Table 1. calculation example with the rod theory and the BEM

Rod theory		BEM		Difference in %	
$\Delta\dot{q}_i$	$\Delta\dot{q}_e$	$\Delta\dot{q}_i$	$\Delta\dot{q}_e$	$\Delta\dot{q}_i$ difference	$\Delta\dot{q}_a$ difference
78.76 W/m^2	7.90 W/m^2	78.74 W/m^2	7.95 W/m^2	0.03%	-0.62%

So far the problem was only considered for homogeneous boundary conditions on both side of the glazing. **Figure 6** shows, how the results can be extended to inhomogeneous boundary conditions. **Figure 6 (a)** represents the case that there is no activation in the glazing. This is referred to as the passive state (index 0). The passive level t_{m0} is given by

$$t_{m0} = \frac{R_i\, t_e + R_e\, t_i}{R_i + R_e}\,. \tag{12}$$

This temperature can be easily derived from the equivalent electrical circuit shown in **Figure 6 (a)**. **Figure 6 (b)** is exactly same as **Figure 5** (c). This temperature field is referred to as the thermal activation (prefix Δ). With the activation, the glazing turns into an activated state, which is shown in **Figure 6 (c)**.

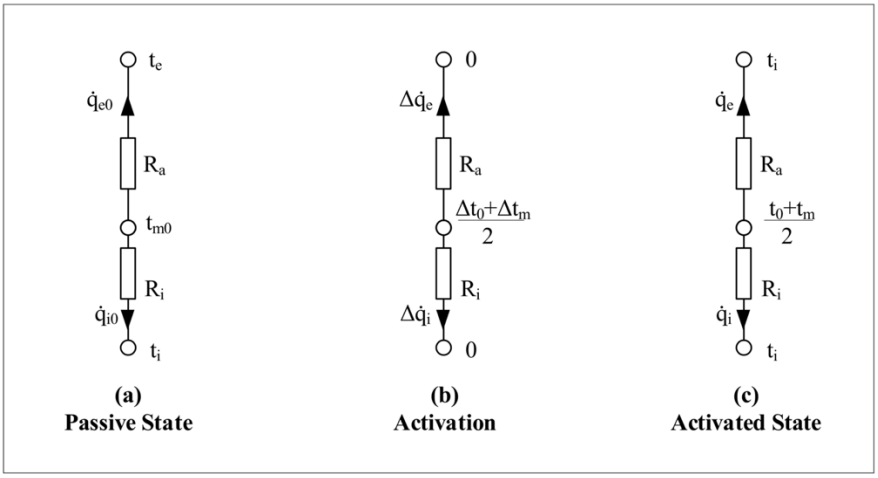

Figure 6. rod theory for thermal activated slabs

Due to the superposition principle, the field of the activated state is the sum of the fields of the passive state and of the activation. This also holds for the heat flows. Values of interest are particularly

$$\frac{t_0+t_m}{2} = t_{m0} + \frac{\Delta t_0+\Delta t_m}{2}\,, \tag{13}$$

$$\dot{q}_i = \dot{q}_{i0} + \Delta\dot{q}_i\,, \tag{14}$$

and

$$\dot{q}_e = \dot{q}_{e0} + \Delta\dot{q}_e. \tag{15}$$

In cases with two thermal activated panels as in figure 2 (c), the superposition principle remains also applicable. With the one-dimensional simplified model and the superposition principle, the most complex part of the heat conduction becomes lean enough to use it for the further modelling.

4. Modelling the combined temperature and flow rate distribution inside the window

If the capillary glass panel is used for thermal energy harvesting for heat pumps during the heating period, the fluid temperature will be close to the ambient air temperature. However, the fluid viscosity becomes higher at lower temperature. As a result, the flow rate in the capillary fluid channel decreases, which leads in even lower fluid temperature. This could cause stagnation, which means the fluid flow is frozen in the critical region. **Figure 7** shows the kinematic viscosity of the fluid

Antifrogen L with volume concentration of 47% from the manufacturer Clariant, which was used in the prototype. To avoid the stagnation, it's necessary to model the temperature and flow rate distribution inside the window.

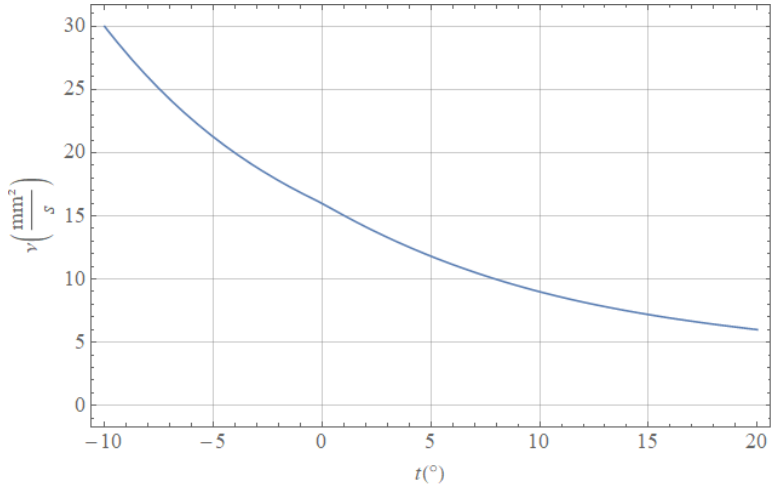

Figure 7. Kinematic viscosity Clariant Antifrogen L, concentration 47 Vol. -% [7]

Modelling the temperature and flow distribution inside the glazing requires the consideration of the temperature dependency of the viscosity. There are strong interferences between temperature and flow distribution because of this dependency. Therefore, the capillary fluid channels have to be discretized into several sections. Moreover, each capillary fluid channel has different flow rate and temperature, depend on its difference to the supply and return connectors of the glazing. Furthermore, the stems also have to be divided into sections for each capillary fluid channel.

Figure 8 shows a full-scale model with maximum number of sections **(a)** along with distributions of the temperature **(b)** and of the flow **(c)**, which are calculated with this model. Whereas the temperature differs in each section of a capillary fluid channel, the flow differs only between the capillary ducts and decreases from left to right. The critical region of the glazing is the top right part, which is the return of the outermost capillary fluid channels, as shown in **Figure 8**.

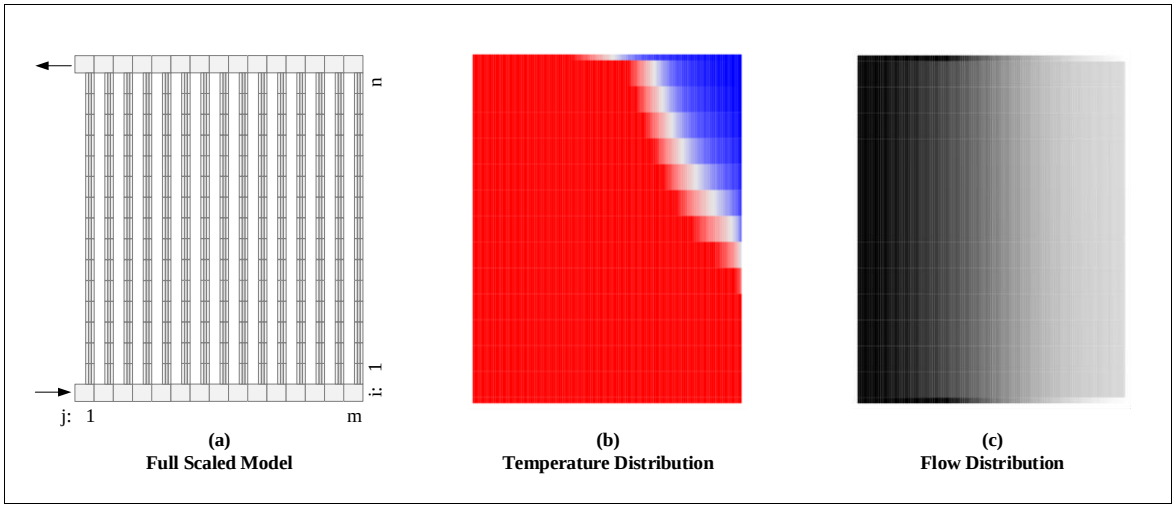

Figure 8. full scaled model for combined heat and mass transfer inside the glazing

High number of sections will increase the computing time. In order to prove whether the stagnation occurs and limit the computational complexity, we define a hydraulic resistance k. Since the fluid flow in the capillary glass device remains laminar at even high flow rate, thus we define the hydraulic resistance k-value as

$$k = \frac{\Delta p}{\dot{V}}. \tag{16}$$

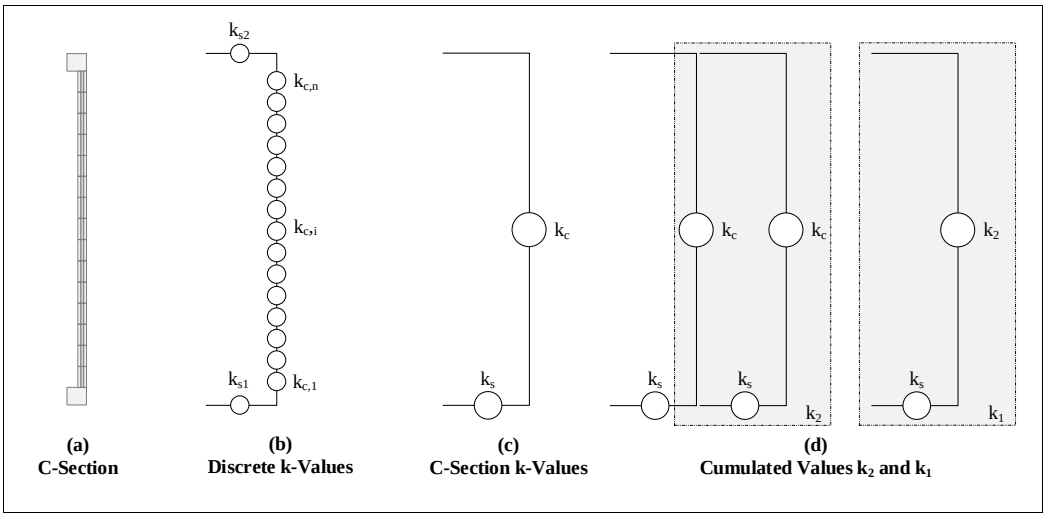

Figure 9. Using k-values for fast hydraulic calculation

As stated in the previous section, low fluid temperature and low flow rate causes stagnation. The numerical simulation shown in **Figure 8** confirms that the stagnation occurs in the outermost capillary fluid channels. With this knowledge, some simplification can be made. Firstly, the capillary glass panel can be divides into lots of C-shape sections, which contains one fluid channel and the supply and return water stem element connected to this channel. For the outermost channels, a fine discretization of the fluid channel is necessary, as shown in **Figure 9** (a). For each discretized section and the stem element, we calculated both the temperature and the k-value, as shown in **Figure 9** (b). For the non-critical region, a fine discretization is not necessary. Therefore, we may treat one fluid channel as a whole section and determine the hydraulic resistance k-value for the fluid channel (k_c) and the stem element (k_s), as shown in **Figure 9** (c). Since the fluid channels in the non-critical region don't require discretization, the hydraulic resistance k-values of the non-critical regions can be combined together, similar to the parallel connection of electrical resistances, as shown in **Figure 9** (d).

This simplification enables fast hydraulic and thermal calculation, which is useful for the combination of other models such as heat pump model to determine the heat harvesting and estimate the energy efficiency.

5. Further modelling for device performance estimation

Based on the combined application shown in **Figure 2** (c), we also considered another interesting application for the capillary glass panel. Instead of connecting both capillary glass panels to a central heat pump with pipes throughout whole building, the triple glazed device can be directly as a decentral heat pump for heating and cooling with a direct current compressor and an expansion valve. Moreover, the thermal insulation in the device can be overbridged by circulating the refrigerant in the inner and outer capillary glass panel with a hydraulic pump. This concept is useful in the trans-seasonal period, increasing heat dissipation from the indoor to the environment. Optionally, the mid glass panel can be coated with an a-Si thin film [9], turning into a semi-transparent photovoltaic. The electricity generated from the semi-transparent photovoltaic can compensate the electrical energy consumption of the on-device compressor and the hydralic pump, or can be stored for other application such as indoor lightning. **Figure 10** (a) shows the concept and the necessary components of this device. The detailed introduction can be found in [1].

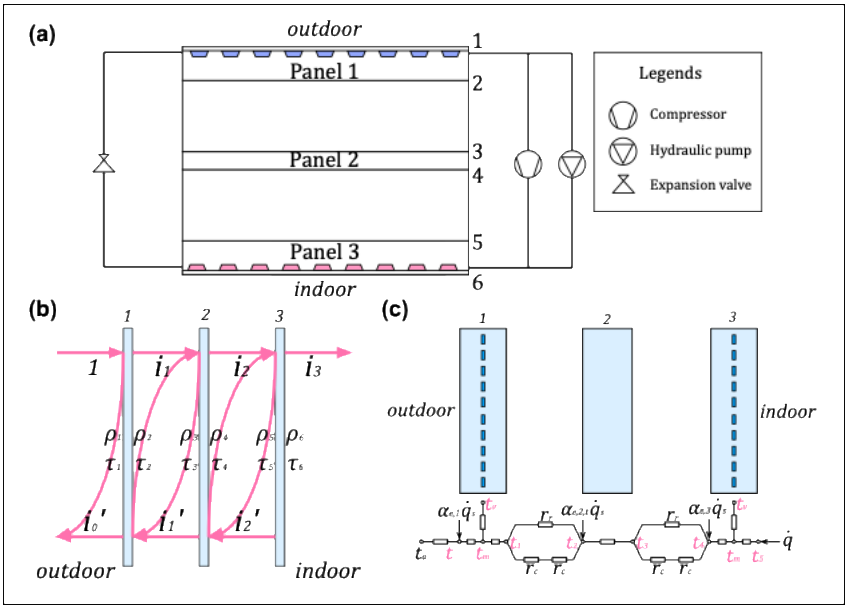

Figure 10. (a) multifunction triple glazed device with capillary glass panel (b) simplified optical model according to ISO 9050 [10], VDI 6007 part 2 [11] (c) simplified thermal model [1]

When evaluating the device energy efficiency, it's important to determine the amount of the electricity generated by the semi-transparent photovoltaic panel. Furthermore, it's well-known that the photovoltaic transfer efficiency is temperature dependent. Therefore, a simplified device optical model and a simplified device thermal model are required.

We adopted the concept from the international standard ISO 9050 and the German standard VDI 6007 part 2 for the device optical modelling [10] [11]. Instead of calculating the infinite reflection between surfaces, this model considers the total outgoing radiation from one surface to another. Using this method, the effective reflectance, transmittance of the triple glazed device and the absorptance of each glass panel can be determined, as shown in **Figure 10** (b). It needs to be noticed that for both capillary glass panels, the absorbed irradiation turns into heat eventually, while the absorbed irradiation of the semi-transparent photovoltaic panel turns into heat and electricity. Therefore, the effective thermal absorptance of the photovoltaic panel $\alpha_{e,2,t}$ should also be modified as

$$\alpha_{e,2,t} = \alpha_e - i \cdot \eta \tag{17},$$

where α_e is the effective absorptance of the semi-transparent photovoltaic panel, i is the percentage of solar irradiation absorbed by the panel and η is the photovoltaic transfer efficiency. The transfer efficiency can be estimated with a simplified linear model [12]

$$\eta = \eta_{ref} \cdot [1 - \beta(t_p - t_{p,ref})] \tag{18},$$

where the η_{ref} is the reference transfer efficiency of the photovoltaic panel, β is the linear coefficient, t_p is the panel temperature and $t_{p,ref}$ is the reference panel temperature.

The thermal model derives from the German standard VDI 6007 part 2 and the European standard EN 673 [11] [13]. This model can be presented with an equivalent R-network, as shown in **Figure 10** (c). In this model, the convective heat transfer between the panel surface and the filled gas within cavity is considered with a simplified heat transfer coefficient described in [11]. The radiant heat exchange between panel surfaces is treated as the case of two infinite parallel plates. To calculate the heat dissipation and absorption of the capillary glass panels, we adopted the rod theory model described in Section 2.

The simplified optical and thermal model allows coupling with a room or building thermal model to evaluate the thermal performance and the device energy efficiency with relatively short computing

time. We used this model to simulate rooms with different size ratios and different internal heat gain, the result discussion can be found in [1].

6. Conclusions

To estimate the performance of the capillary glass panels, different calculation models are needed. We developed different simplified models to calculate the heat flux, the temperature and the flow rate distribution. Simplified models shorten the computing time but still provide satisfactory accuracy, which enables flexible and fast performance and efficiency estimation of different applications for the capillary glass panel.

References

[1] Su L, Fraaß M, Kloas M, Wondraczek L 2019 *Performance Analysis of Multi-Purpose Fluidic Windows Based on Structured Glass-Glass Laminates in a Triple Glazing* (*Frontier in Materials vol 6*) DOI: 10.3389/fmats.2019.00102
[2] Heiz B P V, Pan Z, Lautenschläger G, Sirtl C, Kraus M, Wondraczek L, 2016 *Ultrathin Fluidic Laminates for Large-Area Façade Integration and Smart Windows* (*Advanced Science vol 4*) DOI: 10.1002/advs.201600362.
[3] Jaswon M A and Symm G T 1972 *Integral equation methods in potential theory and elastostatics* (London, New York: Academic Press)
[4] Brebbia C A, Telles J C F and Wrobel L C 1984 *Boundary element techniques: theory and applications in engineering* (Berlin, Heidelberg, New York, Tokyo: Springer-Verlag)
[5] Carslaw H S and Jaeger J C 1959 *Conduction of Heat in Solids* (Oxford: At the Clarendon Press)
[6] Kalous K 1937 *Allgemeine Theorie der Strahlungsheizung (Forsch Ing-Wes* vol 8*)* pp 170-183
[7] Antifrogen Calculator: https://www.clariant.com/en/Business-Units/Industrial-and-Consumer-Specialties/Heat-Transfer-Fluids/Calculator, accessed Feb. 01, 2016
[8] Fraaß M 2004 *Numerische Leistungsbestimmung thermisch aktivierbarer Bauteile mittels des Randelementenverfahrens (BEM)(Gesundheitsingenieur)*
[9] Chae Y T, Kim J, Park H, Shin B 2014 *Building energy performance evaluation of building integrated photovoltaic (BIPV) window with semi-transparent solar cells* (*Applied Energy. 129 217–227*) DOI:10.1016/j.apenergy.2014.04.106.
[10] ISO 9050 2003, *Glass in building - Determination of light transmittance, solar direct transmittance, total solar energy transmittance, ultraviolet transmittance and related glazing factors*
[11] VDI 6007 Blatt 2 2012, *Calculation of transient thermal response of rooms and buildings - Modelling of windows*
[12] Evans D L 1981, *Simplified method for predicting photovoltaic array output (Solar Energy. 27 555–560)* DOI:10.1016/0038-092X(81)90051-7.
[13] BS EN 673 2011, *Glass in building - Determination of thermal transmittance (U value) - Calculation method*

Acknowledgments

We gratefully acknowledge financial support from the European Commission through its Horizon-2020 framework program (Grant Agreement No. GA 637108) as well as fruitful discussion and collaboration with all members of the LaWin project consortium.